MOVING GRATE COMBUSTION OPTIMISATION WITH CFD AND PIV

Thomas Nussbaumer[1,2], Martin Kiener[1]
[1]Lucerne University of Applied Sciences, CH - 6048 Horw, Switzerland, www.hslu.ch
[2]Verenum Research, Langmauerstrasse 109, CH - 8006 Zurich, Switzerland, www.verenum.ch

ABSTRACT: Grate boilers are often applied for biofuels with high ash and moisture content. In heating applications, part load operation often occurs. The paper presents measures to optimise the fluid dynamics in moving grate boilers to improve the part load capability. For this purpose, the secondary air injection and obstacles in the combustion chamber are investigated by Computational Fluid Dynamics (CFD) and validated by model experiments with Particle Image Velocimetry (PIV). The most promising concepts are implemented in a 1.2 MW boiler and experimentally validated. The results show that the combustion quality can be improved by a factor of 4 compared to a reference case with already low emissions. In addition, the boiler can be operated at lower excess air ratio, which enables an efficiency increase. By implementation of the presented measures, a stable operation from little below 30% load to full load can be achieved with CO emissions below 15 mg/m_n^3 at 11 Vol.-% O_2 at an excess air ratio of 1.8. However, beside optimum fluid dynamics, undisturbed grate coverage is advantageous to achieve good combustion quality.
Keywords: Grate combustion, part load, modelling, emissions.

1 INTRODUCTION

1.1 Grate boiler applications

Moving grate boilers as in Fig. 1 are widely applied for biomass fuels with high ash and moisture content in typical applications from 0.5 – 25 MW [1].

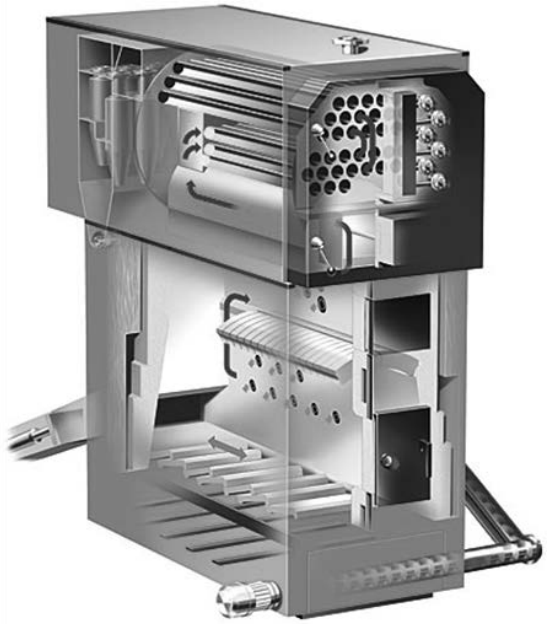

Figure 1: Layout of a moving grate boiler (picture: Schmid AG energy solutions).

High combustion quality for flue gas and grate ash is usually achieved at full load operation. Nowadays boilers also work in part load conditions, however mostly only above 50% of nominal output. Lower loads lead to intermittent on/off operation which leads to higher emissions. In addition, particle removal devices, i.e., electrostatic precipitators (ESP) or fabric filters are often bypassed or in off-mode during the start-up phase in order to avoid damage through condensation [2]. Furthermore part load operation or changing fuel properties (e.g. lower moisture content, different bed porosity) can lead to uneven fuel distribution on the grate e.g. with uncovered grate sections in the second part of the grate. This can result in leaking primary air (LPA), uncontrolled flow conditions in the freeboard above the grate and in streaks with increased excess air and reduced temperatures and therefore leads to higher CO-emissions [3].

1.2 Target

The aim of the present work is the development of aerodynamic measures which enable to extend the part load range. Thereby stable operation from 30% to 100% of the nominal load in compliance with emission regulations and at low excess air ratio and high efficiency shall be achieved.

2 NUMERICAL DESIGN OPTIMISATION BY CFD

2.1 Method

The fuel conversion on the grate is calculated in a one-dimensional transient integral model in adaptation to [4]. The conversion from wet wood to water vapour and pyrolysis gases consisting of CO, CO_2, H_2, H_2O, CH_4, O_2 und N_2 is modelled as function of the local excess air ratio on the grate. For the simulation of the fluid flow ANSYS CFX is applied using a k-ε description of the turbulence and applying the gas phase reactions for CO burnout based on the Eddy Dissipation Model EDM [5, 6]. The calculations are performed with an EDM factor of A = 1, a minimum reaction temperature of $T_{R,min}$ = 873 K, and under the assumption of symmetric flow conditions [7]. As boundary condition the parameters according to Table 1 are assumed.

Table 1 Assumptions for CFD modelling

Thermal firing capacity	1.4 MW
Boiler capacity	1.2 MW
Boiler efficiency	85%
Fuel moisture content	50%
Primary and secondary air temperature	80°C
Excess air ratio	
Primary air = λ_{PA}	0.72
Secondary air 1 = λ_{SA1}	0.86
Secondary air 2 = λ_{SA2}	0.22
Total excess air: $\lambda_{tot} = \lambda_{PA} + \lambda_{SA1} + \lambda_{SA2}$	1.80

For the investigated geometries and operating conditions, the fluid flow is characterised by the Reynolds number and the impulse ratio between the jet flow and the main flow. The Reynolds number as ratio between inertia forces and viscous forces of the flow describes the degree of turbulence:

$$Re = \frac{u \cdot L}{\nu}$$

u = velocity [m/s]
L = length [m]
ν = kinematic viscosity [m^2/s]

In the present application, mixing effects between two fluid flows, here combustible gases and air, are of specific interest. The situation in the combustion chamber can be described as a jet in cross flow (JICF) [8,9]. The mixing of a JICF with the main flow is strongly influenced by the impulse ratio IR between the two flows. For the secondary air, IR is defined as ratio of the *impulse current density* (not the impulse) of the jet flow to the one of the main flow:

$$IR_{JM} = \sqrt{\frac{\rho_J \cdot u_J^2}{\rho_M \cdot u_M^2}}$$

u_J velocity of jet flow [m/s]
u_M velocity of main flow [m/s]
ρ_J density of jet flow [kg/m^3]
ρ_M density of main flow [kg/m^3]

In order to compare different secondary air nozzle arrangements the impulse ratio normed for the reference case ir_{norm} is introduced:

$$ir_{norm} = \frac{IR_{JM}}{IR_{JM\,ref}}$$

To achieve an improved gas phase combustion two different methods are investigated:

Concept 1: Variation of arrangement and diameter of the secondary air nozzles in order to change the scattering of secondary air and the impulse ratio between jet and main flow.

Concept 2: Use of flow obstacles to increase the turbulence.

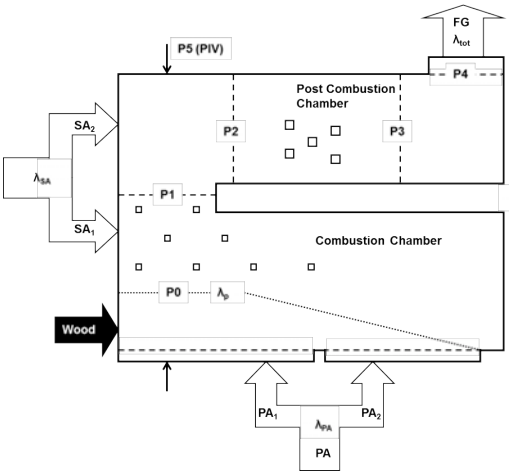

Figure 2: Schematic view of the 1.2 MW moving grate boiler with planes P0 to P4 used for evaluation of CO emissions and mixing efficiencies. The PIV measurements on the scaled model were performed in plane P5.

The analysis of the CFD simulations is performed in four planes [7] by considering carbon monoxide (CO) as indicator of the combustion quality. The mixing efficiency as introduced in [6] as mixing quality is investigated as additional parameter. In order to compare the different layouts the emission values at the exit of the post combustion chamber are used (plane P4, Fig. 2). Additionally the reaction progress over the four planes for evaluation is observed. For the simulations 30 layouts were considered of which some are described below.

2.2 Influence of secondary air injection

Table 2 summarises the results of the CFD simulations for secondary air arrangements SA-1 to SA-9. The values show the CO concentration and the mixing efficiency in plane P4 as well as the pressure loss from the entry to plane P4. Emanating from the reference case firstly the cross section of the secondary air nozzles is reduced. With reduced area the impulse ratio as well as the turbulence level is increased, leading to increased pressure loss. As second step the number of the nozzles is doubled.

The results in Table 2 show that the combustion quality increases with decreasing total cross sectional area of the air injection nozzles as a consequence of increased jet velocity and impulse ratio. This, however, also results in an elevated pressure loss. As a promising alternative, the combustion quality can also be improved by increasing the number of air injection nozzles while maintaining the total cross sectional area and therefore keeping the pressure loss constant.

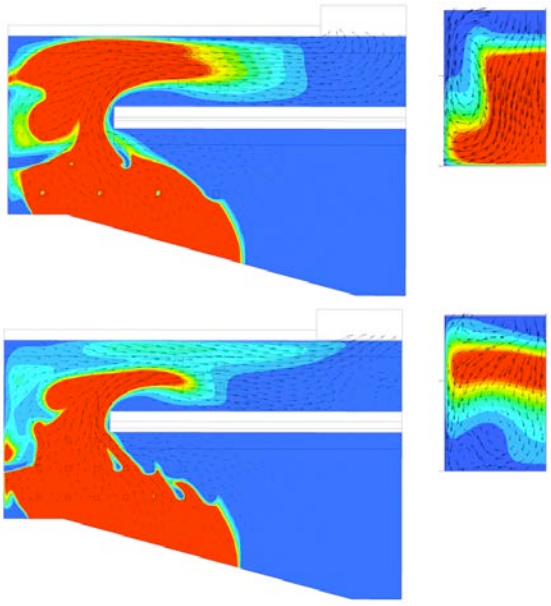

Figure 3: Comparison of reference case (above) and case SA-8 with improved secondary air injection (below) by means of CO concentration (red = high concentration). Left: Combustion chamber and post combustion chamber. Right: Half of plane P4 in more sensitive scale.

Fig. 3 shows the influence on the CO-reduction for the reference case and the case SA-8. The reference case exhibits a streak of high CO concentration flowing into the post combustion chamber. The case SA-8 with doubled number of secondary air nozzles but maintaining the total cross sectional area shows a similar behaviour but with significantly reduced CO streak. This leads to a decrease of the CO concentration in the control plane P4.

Improved gas phase combustion is therefore reached only by improved scattering of secondary air while maintaining the same impulse ratio.

Apart from the reference case, the cases SA-3 und SA-8 with a cross section of the nozzles of 50% are chosen for the experimental validation on a 1.2 MW grate boiler (Table 2). In case SA-3 the nozzle number remains as in the reference case whereas in case SA-8 it is doubled. According to the CFD calculations, these variations promise an improvement of the combustion quality with the same (SA-8) or a slightly increased pressure loss (SA-3). Additionally a compromise case SA-10 is defined in which the nozzle number is increased by 50%, which results in a normed impulse ratio of 1.3 as also here nozzles with halved cross section are used.

2.3 Influence of flow obstacles

Table 3 shows the results of the CFD-calculations for the cases with obstacles in the combustion or post combustion chamber. There is only a minor influence on the pressure loss. Two cases cause a small increase of CO emissions, the other cases exhibit an improved combustion quality by a factor of 2 to 10. However, the cases O-1 and O-6 with a cross section diminution in plane P1 cause unwanted temperature peaks on the front wall. This is confirmed by practical experience with slagging problems in this wall area. Therefore these cases are not implemented in the prototype facility and the cases O-2, O-4 and O-8 are chosen for experimental validation.

Table 2 Values for CO-Concentration, mixing efficiency (ME) and pressure loss (Δp) in plane P4 in comparison to the reference case (= 100%) for different secondary air nozzle arrangements calculated with CFD.

EXP: Cases chosen for experiments
A_D: Nozzle cross section
SA: Secondary air
SA-10: Experimentally investigated case
ME: Mixing efficiency (mixing quality) as introduced in [6].
N: Number of secondary air nozzles
A_{tot}: Total cross sectional area of secondary air nozzles
ir_{norm}: Impulse ratio normed with reference case

Case	EXP	N/N_{ref} [-]	$A_D/A_{D.ref}$ [-]	$A_{tot}/A_{tot.ref}$ [-]	ir_{norm} [-]	CO/CO_{ref} [%]	ME/ME_{ref} [%]	$\Delta p/\Delta p_{ref}$ [%]
SA-1		1	1	0.125	8	0.1	99	6630
SA-2			0.25	0.25	4	2	100	1647
SA-3	+		**0.5**	0.5	**2**	**21**	**101**	**405**
Ref	+		**1**	1	**1**	**100**	**100**	**100**
SA-4			2	2	0.5	252	96	23
SA-5		2	0.0625	0.125	8	0.1	92	6464
SA-6			0.125	0.25	4	0.1	100	1683
SA-7			0.25	0.5	2	3	98	405
SA-8	+		**0.5**	**1**	**1**	**42**	**97**	**97**
SA-9			1	2	0.5	199	95	23
SA-10	+	**1.5**	**0.5**	**0.75**	**1.33**	–	–	–

Table 3 Values for the cases with obstacles compared to the reference case, calculated with CFD.
SA: Secondary air, PCC: Post combustion chamber

Case	EXP	Variation	CO/CO_{ref} [%]	ME/ME_{ref} [%]	$\Delta p/\Delta p_{ref}$ [%]
Ref	+	**No**	**100**	**100**	**100**
O-1		Narrow deflection	26	105	138
O-2	+	**Obstacle middle**	**27**	**103**	**132**
O-3		Obstacle after SA_2	106	99	103
O-4	+	**Obstacle side**	**20**	**106**	**141**
O-5		Asym. obstacle in PCC	57	103	137
O-6		Neck in P1	38	104	113
O-7		Nose before deflection	126	98	97
O-8	+	**Obstacle ceiling**	**11**	**104**	**222**

3 FLUID MODEL EXPERIMENTS WITH PIV

For validation of the CFD simulations, measurements on a 1:13 scale model are performed. By means of similarity it is guaranteed that the model represents the reality in an appropriate way. Apart from geometric similarity, similar turbulence, expressed in terms of Reynolds number, and similar impulse ratios are considered [6].

By adding a tracer in the form of oil droplets and illumination of these droplets by means of a laser sheet in the respective plane, the local velocity can be identified by Particle Image Velocimetry (PIV) [6]. With one single camera in operation the analysis is two-dimensional, by using two cameras the flow can be analysed in three dimensions. Fig. 4 shows the experimental setup while in Fig. 5 CFD-calculations are compared with experimental PIV data. The analysis is performed for plane P5 as defined in Fig. 2. The following trends are found [7]:

- In the CFD-calculations the penetration depth of the secondary air jet is slightly overestimated compared to the experimental data from PIV measurements. Otherwise the CFD calculations and PIV-measurements show good qualitative agreement of the flow situation.
- Moreover, the PIV measurements show that the flow is not completely but nearly symmetric. The assumption of a symmetric flow for the CFD-simulations is therefore justified.

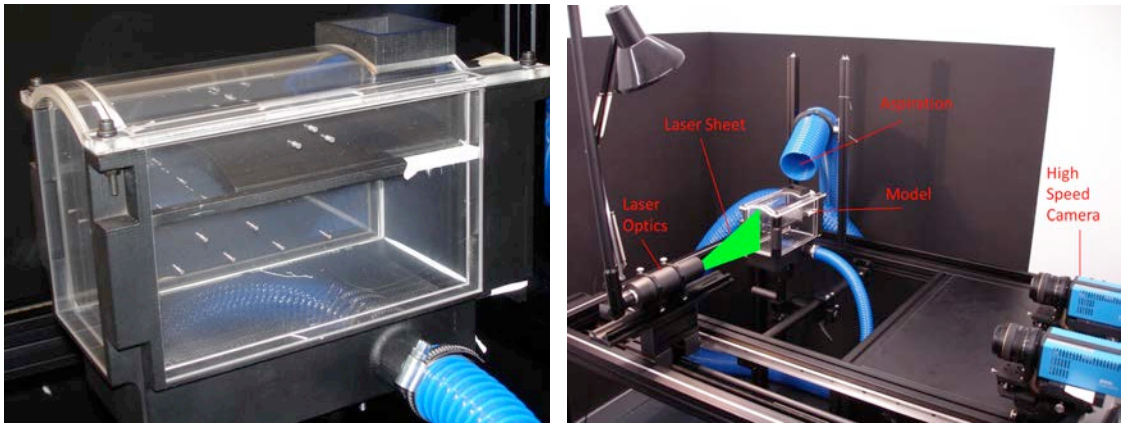

Figure 4: Scaled model (left) and experimental setup for 2D and 3D Particle Image Velocimetry (PIV) (right).

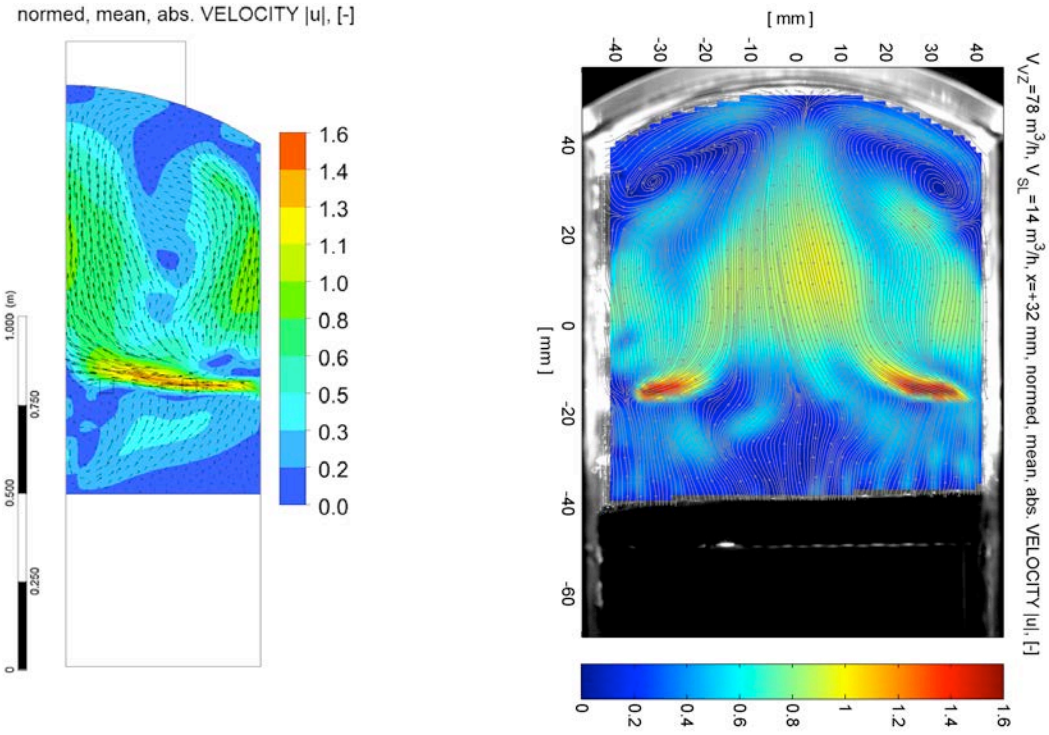

Figure 5: Comparison of CFD-calculations (left) with PIV-measurements on the model (right). The pictures show the normed mean velocity in plane P5 for the reference case. For the CFD-calculation (left) only the right half of the combustion chamber is shown as a symmetric flow is assumed.

4 EXPERIMENTS ON A 1.2 MW BOILER

4.1 Method

For the experiments a 1.2 MW moving grate boiler is used which can be operated with the different arrangements of secondary air injection and flow obstacles. For validation the following measured variables and parameters are used:

- O_2 (paramagnetic), CO_2 und CO (ND-IR)
- Excess air ratio λ_{tot}
- Particulate matter, gravimetric with plane filter
- Temperature of flue gas, post combustion chamber and boiler wall
- Thermal firing capacity
- Combustion efficiency
- Flue gas volume flow (Δp with pitot tube)
- Combustion air volume flow PA_1, PA_2, SA_1 and SA_2 (heated wire anemometry)
- Grate movement and de-ashing movement
- Set value of boiler output.

For each case a mean value of CO concentration over 30 minutes stationary phase, weighted with flue gas volume flow, is considered and compared at total excess air ratio of $\lambda_{tot} = 1.8$ [7].

4.2 Influence of secondary air injection

Table 4 summarises the results. The emission limit value of the Luftreinhalte-Verordnung LRV (ordinance on air pollution control OAPC) of 250 mg/m$_n^3$ at 11 Vol.-% O_2 is clearly undercut for all cases including the reference case. The analysed measures show the same behaviour for full load and part load conditions with the following trends [7], which confirm the CFD-calculations:

- Decreasing of the total cross sectional area of the secondary air nozzles by 50% and therefore increasing the impulse ratio (case SA-3) results in reduction of CO emission of 34%. In the same time the optimal operating point is reached at lower excess air ratio thus resulting in increased combustion efficiency.
- Doubling the number of secondary air nozzles while maintaining the total cross sectional area and hence the impulse ratio (case SA-8) improves the CO-emissions by 62% without increased pressure loss.
- A compromise of both measures with 50% more secondary air nozzles and halved nozzle cross section, resulting in an normed impulse ratio of 1.33 (case SA-10), decreases CO emissions by 74%.

Fig. 6 and Fig. 7 show the measured CO mean values at an excess air ratio of $\lambda_{tot} = 1.8$ as a function of the load. The lowest values for the optimised cases are achieved at loads between 50% and 60% (Fig. 6). The case SA-10 exhibits the best results with CO values below 15 mg/m$_n^3$ in the whole load range (Fig. 6). Therefore this case is termed optimised basis and serves as starting case for the analysis of the influence of obstacles within the post combustion chamber (Fig. 7).

4.3 Influence of obstacles

Starting from the optimised basis case SA-10, all the flow obstacles lead to improved combustion quality at part load but to worse combustion quality at full load (Fig. 7).

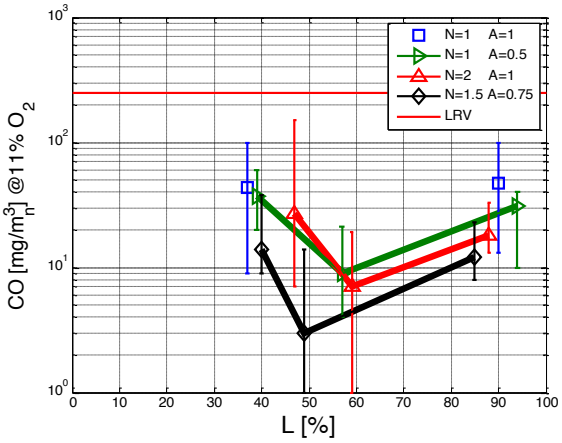

Figure 6: Influence of secondary air injection type on mean CO concentration at $\lambda_{tot} = 1.8$ as function of load L for the following cases:
– Reference case (N=A=1),
– SA-3 (A=0.5),
– SA-8 (N=2) and
– SA-10 (N=1.5, A=0.75).
LRV value = emission limit value of the Luftreinhalte-Verordnung (ordinance on air pollution control).

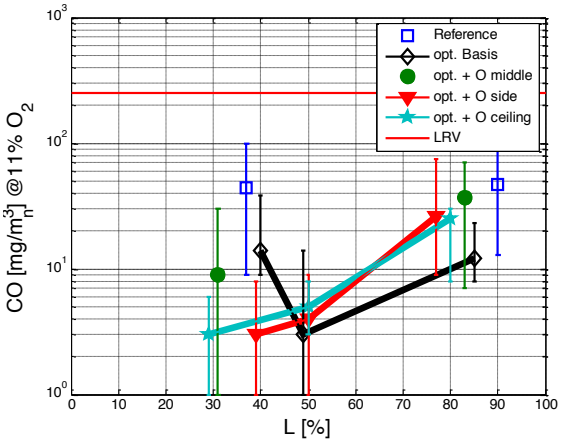

Figure 7: Influence of obstacles on mean CO concentration at $\lambda_{tot} = 1.8$ as function of load L.
Case SA-10 serves as optimised basis which is analysed with additional obstacles in the middle, side, and on the ceiling of the post combustion chamber.
LRV = emission limit value.

5 CONCLUSIONS

- The reference case of the analysed grate boiler already securely meets the emission limit value of CO at nominal load.
- In practical experience an increase of emissions during part load operation is often observed. With the assumption of a completely covered grate, CFD calculations do not show this behaviour. Measurements on the test boiler show that it is possible to reach part load operation below 40% without increase of CO emissions. This however requires a completely covered grate, which is achieved by means of an adequate grate movement and air supply. Uncovered grate sections can lead to an increase in CO emissions [3]. It is therefore assumed that part load difficulties are often due to insufficient grate coverage.
- Starting from an appropriate grate coverage, it is possible to further improve the part load range by means of fluid dynamic measures. As first measure serves an optimisation of the secondary air supply, additionally flow obstacles are possible.
- An improvement of the secondary air injection can either be achieved by increasing the impulse ratio between the secondary air and the main flow (at higher pressure loss) or by increasing the number of secondary air nozzles and therefore improved scattering of the secondary air (at equal pressure loss). A combination of both approaches leads to the best results.
- The CO-emissions are, starting from an already low value, reduced by a factor 4. Thereby it is possible to maintain stable operation conditions from slightly below 30% to 100% of the nominal load. At an excess air ratio of $\lambda_{tot} = 1.8$ CO-emissions below 15 mg/m_n^3 at 11 Vol.-% O_2 over the whole load range are achieved. At the same time the optimal excess air ratio is reduced by 0.2, i.e. from $\lambda_{tot} = 1.7$ to 1.5, thus enabling a higher combustion efficiency [7]. In addition, a more stable operation at part load and with high moisture content is expected.
- The use of CFD is confirmed as an appropriate tool for improving fluid flow design in combustion, while model scale experiments with PIV enable a validation of the quantitative flow situation and are therefore a complementary tool. PIV is of specific interest to identify or confirm special flow effects such as e.g. swirls, transition, turbulence, and symmetry which show a high uncertainty for numeric modelling.
- Apart from that the pyrolysis gas release on the grate is essentially influencing the combustion and has therefore to be considered as well. For this purpose, the solid fuel conversion on the grate is described in a separate model as basis for input data for CFD calculations [10].

6 REFERENCES

[1] S. Van Loo, J. Koppejan, *The Handbook of Biomass Combustion and Co-firing*. 2008: Earthscan, London.

[2] Good, J.; Nussbaumer, T.: Überwachung und Vollzug der LRV für Holzheizungen ab 500 kW, *10. Holzenergie-Symposium*, 12.9.2008, ETH Zürich, 219–256

[3] Kiener, M.; Nussbaumer, T.: Influence of uneven fuel distribution on a grate on gas flow conditions and combustion quality, *20th European Biomass Conference*, 18.–22.6.2012, Milano, 2BO.10.2

[4] Klasen, T., Görner K.: Numerical Calculation and Optimisation of a large Municipal Solid Waste Incinerator Plant, *2nd Int. Symp. on Incineration and Flue Gas Treatment Technologies*, University of Sheffield, UK, 4.–6.7.1999

[5] Magnussen, B. F.; Hjertager, B.H.: On mathematical modeling of turbulent combustion with special emphasis on soot formation and combustion, *Symposium (International) on Combustion*, Volume 16, Issue 1, 1977, 719–729

[6] Baillifard, M.; Casartelli, E.; Nussbaumer, T.: Experimental Investigation of the Fluid Dynamics in Wood Combustion Processes, *16th European Biomass Conference and Exhibition*, Valencia, 2–6 June 2008, ETA-Florence

[7] Kiener, M.; Nussbaumer, T.: Strömungsoptimierung einer Vorschubrostfeuerung mit CFD und PIV, *12. Holzenergie-Symposium*, 14.9.12, ETH Zürich, 53–70

[8] Schlüter, J.U.; Schönfeld, T.: LES of Jets in Crossflow and its Application to a Gas Turbine Burner; *Flow, Turbulence and Combustion*, 65: 177-203; 2000

[9] Suman, M.; DNS and Modeling of Jets in Cross Flow; Thesis, University of Minnesota, USA; 2006.

[10] Martinez, J.; Nussbaumer, T.: A One-Dimensional Transient Solid Fuel Conversion Model for Grate Combustion Optimisation, *21st European Biomass Conference and Exhibition*, Copenhagen, 3–7 June 2013, 2DV.3.61

7 ACKNOWLEDGMENTS

Swiss National Science Foundation SNSF
Swiss Federal Office of Energy SFOE
Commission for Technology and Innovation CTI
SCHMID energy solutions Eschlikon